ESTIMATING THE USEFUL LIFE OF THE SEMPOR RESERVOIR USING EROSION MODELLING

SATRIO BUDIMAN ⓘ , SLAMET SUPRAYOGI ⓘ

Department of Environmental Geography, Faculty of Geography, Universitas Gadjah Mada, Yogyakarta, Indonesia

ABSTRACT: Sedimentation determines how optimal a reservoir functions throughout its design life. The Sempor Reservoir in Central Java, Indonesia, will be 45 years old in 2023. At least 15 million m^3 of particles have been sedimented in the reservoir for >30 years, reducing its function as an irrigation water source to only 60%. Therefore, assessing its performance in providing irrigation water and generating hydropower electricity is essential, given that its design life ends in 2028. This study was conducted to analyse the sedimentation and estimate the useful life of the Sempor Reservoir based on the erosion potential in its catchment area. The potential sedimentation rate was formulated from erosion potential assessed using the universal soil loss equation (USLE) model, sediment delivery ratio (SDR) and trap efficiency (TE). By contrast, the actual sedimentation rate was determined from changes in the dead storage capacity from 2013 to 2023. The interpolation performance evaluation of the bathymetric survey results was tested using the coefficient of determination (R^2), Nash-Sutcliffe efficiency (NSE), and mean absolute percentage error (MAPE) which resulted in values of 0.917; 0.87; and 13.03%, respectively. The results show that the catchment area had an erosion potential of 3,405,353.86 $t·a^{-1}$, resulting in a potential sedimentation rate of 309,106.63 $m^3·a^{-1}$. The calculated actual sedimentation rate was 33,903.28 $m^3·a^{-1}$. Therefore, the useful life of the Sempor Reservoir was estimated to end in 0.5 years and 4.59 years based on the potential and actual sedimentation rates, respectively.

KEY WORDS: bathymetric survey, erosion potential, reservoir, sedimentation rate, useful life

Corresponding author: Slamet Suprayogi; ssuprayogi@ugm.ac.id

Introduction

Currently, managing water resources of different quality, quantity and distribution has become a priority issue (UN Statistics Division 2017). Constructing reservoirs to control floods during rainy seasons and provide water during dry seasons can reduce the annual imbalance of water resources (Indonesia Ministry of Public Works and Settlement 2017). However, reservoirs in tropical areas face intensive sedimentation of insoluble particles (Nagle et al. 1999) mainly sourced from soil erosion in their catchment areas (Marhendi 2013). Sedimentation is the main factor threatening the sustainability of the function and capacity of a reservoir (Haregeweyn et al. 2012). Reduced functions are a severe problem that can hamper

sustainable energy and food production (Schleiss et al. 2016).

Kebumen District has become a buffer zone for rice production in Central Java (Kebumen Agriculture and Food Service Office 2021). The Sempor irrigation area plays a role in irrigating agricultural land, making it is one of the supporters contributing to the success of Kebumen District in serving as a buffer for rice production. However, the Sempor Reservoir received up to 15 million m^3 of particles due to sedimentation from 1978 until 2015 (BBWS Serayu Opak 2020), reducing its function as an irrigation water source to 60%.

Sedimentation is closely related to erosion within a watershed. Indonesia, as a tropical country, has a high risk of erosion due to its

mountainous topography and high rainfall intensity (Wantzen, Mol 2013). In addition, another cause of the high risk of erosion in Indonesia is agricultural land cultivation that does not pay attention to soil and water conservation principles (Sumiahadi, Acar 2019). One of the activities that support the acceleration of sedimentation of the Sempor Reservoir is the emergence of agricultural land in the green belt of the Sempor Reservoir, as shown in Figure 1.

Tillage of agricultural land can lead to the release and separation of soil particles when exposed to raindrops (Ahmad et al. 2020). The material resulting from the release and separation of the soil particles will directly enter the Sempor Reservoir. This is one of the contributors to sedimentation in the Sempor Reservoir. Meanwhile, the catchment area will also contribute to erosion, which will later enter the reservoir as an outlet. Soil erosion in a catchment area produces grains of different sizes, which are the main contributing or determining factor of total sediments that enter a reservoir (Li et al. 2014).

Erosion hazard levels can be assessed using the universal soil loss equation (USLE) model. The USLE is one of the empirical models that are widely used to estimate erosion potential in a watershed. The USLE is designed to predict erosion rates over a long period (Wischmeier, Smith 1978) by drawing on interactions assumed to occur between several parameters in the catchment area to simulate erosion processes (Patil 2018). These parameters are rainfall, soil, slope length and steepness, and land use.

Nevertheless, not all particles from the eroded catchment area are deposited at the outlet. Particles experiencing and completing the sedimentation process at this point of interest are referred to as sediment yield. Sediment yield can be determined using the sediment delivery ratio (SDR), which compares the total sediment accumulating at the catchment outlet with gross erosion in the entire catchment (El-Swaify et al. 1982). Sedimentation occurs when solid particles are moved or transported from the original source (upper reach) to a lower point or outlet (lower reach) (Lihawa 2017). However, particles that are transported to a reservoir are not entirely deposited. The fraction of the deposited particles depends on the reservoir's ability to trap

Fig. 1. Agricultural activities around the inlet of the Sempor Reservoir.

and hold sediments, called trap efficiency (TE) (Subramanya 2008). Identifying TE helps predict the accumulation of deposits entering a reservoir (Dargahi 2012).

Reservoirs are designed with a limited time during which they can perform their functions properly. The duration in which reservoirs have optimal storage capacity in providing services or being used according to their main purpose at the time of construction is called useful life (Sisinggih et al. 2021). The useful life of a reservoir is ultimately determined by soil erosion and sedimentation in a catchment (Gill 1979). Uncontrolled sedimentation rates produce more solid particles that fill the dead storage capacity faster, shortening the useful life of a reservoir than its original design life. Dead storage capacity can be measured with echo sounding using an echosounder, a tool used to record the depth of a water body. An echosounder utilises a transmitter and a transducer to send pulses of sound vibration underwater and receive the echo reflected by the bottom of the water (Nugraha et al. 2013).

The Sempor Reservoir was planned to have a useful life of 50 years (Julia 2017). In 2023, the reservoir will be 45 years old or only five years from the end of its design life. Therefore, it is necessary to determine the remaining useful life of the reservoir using erosion and sedimentation studies. Accordingly, this research aimed to analyse the sedimentation and estimate the useful life of the Sempor Reservoir based on erosion potential.

Materials and method

Study area

The Sempor Reservoir is located in Kebumen District, Central Java, Indonesia. The Sempor Reservoir catchment area is included in the South Serayu Mountains zone. Physiographically, the South Serayu Mountains are included in the anticlinorium zone, which is a series of structural hills (Van Bemmelen 1949). The Sempor Reservoir Catchment Area includes the Karangsambung Formation, Penosogan, Halang, Waturanda and Watuaranda Tuff.

The Sempor Reservoir has an inundation area of ±2.3 km² and a catchment area of 40.63 km².

This reservoir supplies agricultural irrigation with a service area of 6,478 hectares and drinking water, generates hydropower electricity, controls flooding from the Jatinegara River and is utilised for tourism and inland fisheries (Fig. 2).
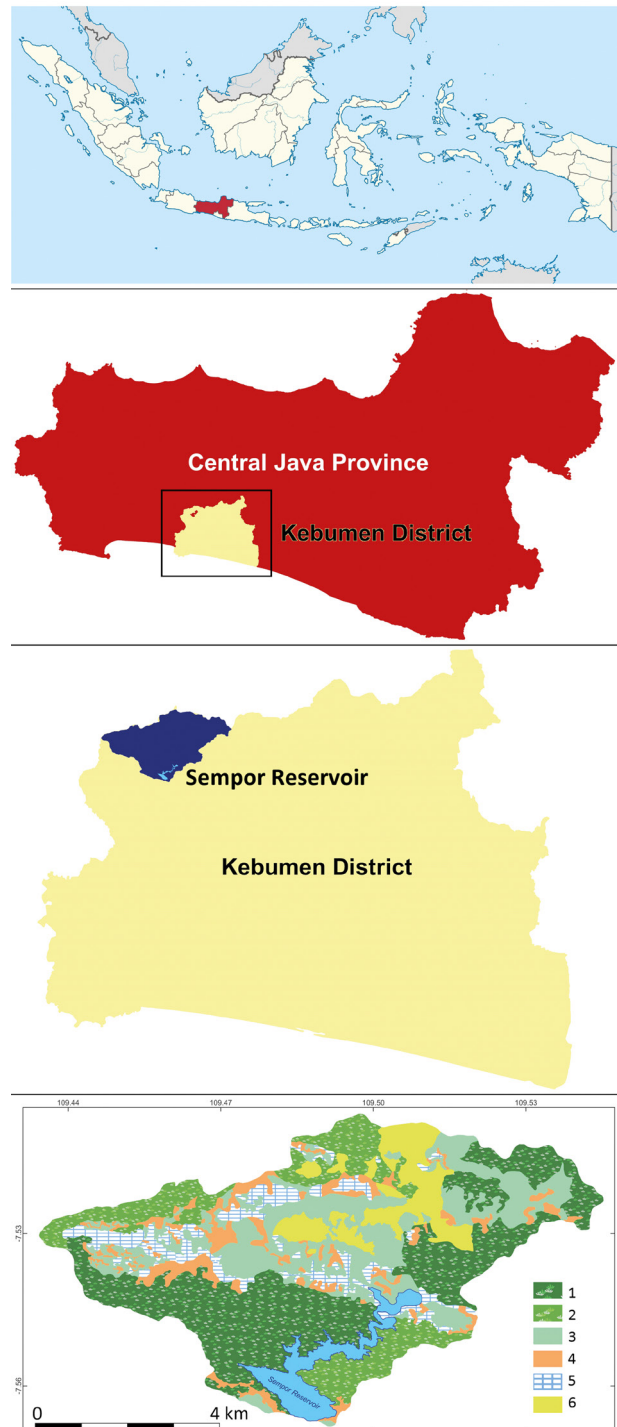

Fig. 2. Study area. Legend for land cover: 1 – conservation forest, 2 – plantation forest, 3 – mixed cropland, 4 – settlement, 5 – paddy rice, 6 – dryland farming.

Land use of the Sempor Reservoir Catchment Area is dominated by forests, both conservation and plantation forests with a fairly homogeneous pattern. Meanwhile, the central part of the catchment area has quite complex land-use variations. Paddy rice and settlements tend to dominate in the western part, which is a colluvial plain. Meanwhile, mixed cropland and dryland farming dominate in the central and northern parts, which are a complex of slightly sloping to steep hills. Mixed cropland in the Sempor Reservoir Catchment Area is generally planted with bamboo, banana, coconut and papaya. Meanwhile, dryland farming is dominated by cassava.

Data collection

The data used in this research were obtained from official institutions and field surveys, as described in Table 1.

Table 1. List of data used in this study.

Data	Data source
Depth of reservoir (2023)	Field survey
Sediment's specific gravity (2023)	Field survey
Digital elevation model	Indonesia Geospatial Information Agency
Land-use data (2020)	Indonesia Geospatial Information Agency
Rainfall data at Sempor, Sampang, Somagede and Kedungwringin Stations (2009–2020)	Water Resources Management Center for Progo-Bogowonto-Luk Ulo; Main Station of Serayu-Opak River Basin

Data analysis

The USLE model was employed to estimate potential erosion rates by integrating four influencing parameters to simulate erosion in a catchment. The parameters used in this study are limited to only a few years due to the unavailability of data from the responsible authorities. The USLE was computed using the following formula:

$$Ea = R \times K \times LS \times CP$$

where:
- Ea is erosion potential ($t \cdot a^{-1}$),
- R is rainfall erosivity (MJ mm ha^{-1} h^{-1} a^{-1}),
- K is soil erodibility ((t ha h)(MJ^{-1} mm^{-1})),

- LS represents the slope length and steepness factors (dimensionless),
- CP combines vegetative cover or crop management with support practices like soil conservation (dimensionless).

Rainfall erosivity (R) factor

Rainfall erosivity (R) plays a crucial role as the primary driver of erosion in that it directly affects the breakdown of soil aggregates (Oliveira et al. 2012). To spatially analyse the R factor in the Sempor Reservoir Catchment Area, data were obtained from four rain gauge stations: Kedungwringin, Sampang, Sempor and Somagede. In addition, the recorded rainfalls were analysed temporally on a monthly basis from 2009 to 2020 to determine the average condition of rainfall in the study area. The Thiessen polygon method was used to determine the station's area of influence based on rain gauge positions and observed rain depths. This method is particularly used in areas with low rain gauge network density (Goovaerts 2000). The R factor was calculated using the Bols equation. According to the Indonesia Ministry of Forestry (2009), the equation is considered representative as it has a good correlation to the incidence of soil loss in Java Island. The formula is suitable for use in areas that have a wet climate.

$$R = 6.119 \times P^{1.211} \times D^{-0.474} \times MaxP^{0.526}$$

where:
- P is the average monthly rainfall (cm),
- D is the number of rainy days in a month,
- MaxP is the maximum rainfall in a month (cm).

Soil erodibility (K) factor

Soil erodibility (K) is defined as the reaction of soil particles to the process of detachment and transport by raindrops or runoff (Renard et al. 1997). It is difficult to determine soil erodibility due to the numerous influencing factors involved, including the spatial variations and dynamics of soil properties and human activities (Yang et al. 2018). For the Sempor Reservoir Catchment Area, the K factor was determined based on landform units from which soil samples were collected.

The landform units were demarcated using pedogeomorphological approaches, which describe the strong correlation between landform and soil morphological properties (Christanto et al. 2018, Reddy et al. 2003). For instance, soils on sloping and flat terrains are formed through different processes (Gerrard 1981), resulting in divergent soil characteristics, particularly permeability (Putri et al. 2017). Besides, landforms are the best reference and indicator in areal delineation (Park, Burt 2002) due to their low temporal variations (Keshavarzi et al. 2019). The K factor was determined using the formula from Wischmeier and Smith (1978).

$$100K = [2.713\ M^{1.14} \times 10^{-4} \times (12 - a)] + [3.25 \times (b - 2)] + [2.5(c - 3)]$$

with M (particles percentage),

$$M = (\%\ \text{slit} + \%\ \text{sand}) \times (100\% - \%\ \text{clay})$$

where:
– a is organic matter content (%),
– b is soil structure code,
– c is soil permeability code.

Slope length and steepness (LS) factor

Slope configuration substantially determines the erosion rate as it influences the quantity and velocity of water flows, the major driver of erosion, which segregate soil particles (U.S. Department of the Interior 2006). Slope data were derived from the country's digital elevation model (The National DEM). LS values were classified according to Regulation No. P.7/DAS-V/2011 issued in 2011 by the Indonesia Ministry of Forestry (2011) on Technical Guidelines for the Standard Operating Procedure (SOP) System for Flood and Landslide Mitigation.

Crop management-soil conservation (CP) factor

The crop management (C) factor shows the effect of vegetation presence and soil surface conditions on total soil loss. The soil conservation (P) factor represents human interventions that can affect erosion processes. Information on CP was derived from land-use data (Asdak 2020). The data used are land use in the year 2020 sourced from the Indonesia Geospatial Information Agency (BIG). CP values of different units of land use were classified according to Arsyad (2010). This classification is the one most closely resembling land use in the study area.

Sedimentation rate

The fraction of solid particles that are transported into the reservoir and deposited at the bottom can be identified using the TE formula. After studying various TE approaches for several reservoirs on Java Island, where the Sempor Reservoir is, Susilo (2001) found that the modified Brune formula had the smallest difference index when compared to the observed data. Therefore, it is also the most suitable for the Sempor Reservoir.

The amount of sediment entering the reservoir, termed sediment yield (G), strongly depends on total soil loss in the catchment area. To determine G, erosion potential calculated by using the USLE was multiplied by the SDR. In a study by Olii et al. (2018), the Sempor Reservoir had a mean SDR of 0.2, with high accuracy ($R^2 = 0.96$) and a low rate of error (0.2%), which can thus be used for further analysis. Table 2 shows the formulas used for TE (modified Brune formula) and G.

Table 2. Parameters for sedimentation rate formulation.

Parameter	Equation
Trap efficiency TE [%]	$TE = \dfrac{96.67 + (17.82 \times (\ln\frac{C}{I})) + (0.569 \times (\ln\frac{C}{I})^2)}{1 + (0.154 \times (\ln\frac{C}{I})) + (0.0153 \times (\ln\frac{C}{I})^2)}$
Sediment yield G [t·a^{-1}]	$G = SDR \times Ea$

where:
– C is the reservoir's capacity (m^3),
– I is the reservoir's inflow discharge (m^3·a^{-1}),
– SDR is sediment delivery ratio,
– Ea is erosion potential based on the USLE model (t·a^{-1}).

Interpolation performance evaluation

Interpolation produces simulated or predicted values, which should be compared with the data measured in the field (observed values). In this research, the comparison was made with cross-validation by removing some sample points (observed values) and using the remaining sample points to project the value at the location of the removed ones (predicted values) (Chang

2007). The recommended tests for hydrological modelling are simple regression analysis or coefficient of determination (R^2), Nash–Sutcliffe efficiency (NSE) and mean absolute percentage error (MAPE) (Moriasi et al. 2007, Tian et al. 2018), as follows:

$$R^2 = \frac{[(n)(\sum op) - (\sum o)(\sum p)]^2}{[(n)(\sum o^2) - (\sum o)^2][n(\sum p^2) - (\sum p)^2]}$$

$$NSE = 1 - \frac{\sum_{i=1}^{n} (o_i - p_i)^2}{\sum_{i=1}^{n} (o_i - \bar{o}_i)^2}$$

$$MAPE = \frac{100}{n} \sum_{i=1}^{n} \frac{|o_i - p_i|}{o_i}$$

where:
– n is the sample depth data,
– o is the observed depth data (from echo sounding measurement),
– p is the predicted depth data (from interpolation).

Useful life determination

The bathymetric survey results in 2023 were used to determine the reservoir's capacity using the Frustum formula, as follows:

$$V = \frac{1}{3} \times H \times (A_n + A_{(n+1)} + \sqrt{A_n \times A_{(n+1)}})$$

where:
– H is the contour interval (m) and
– A is the area between two contours (m^2).

This capacity was later used to calculate the remaining useful life of the reservoir (ΔC) using the Gill (1979) approach, as follows:

$$\Delta C = \frac{G \times TE \times \Delta t}{\gamma}$$

where:
– ΔC is the remaining dead storage capacity at the present time (m^3),
– C is the reservoir's capacity (m^3),
– G is the sediment yield ($t \cdot a^{-1}$),
– TE is the trap efficiency (%),
– Δt is the useful life of reservoir (years),
– γ is the sediment's specific gravity ($t \cdot m^{-3}$).

The sediment's specific gravity (γ) was determined by laboratory tests. Therefore, the sedimentation rate can be defined by dividing between G and γ. ΔC represents the dead storage capacity known through the echo sounding survey conducted in the year 2023 due to limited data of initial reservoir capacity and sedimentation rates from related institutions.

Results and discussion

Erosion potential

Table 3 shows the rainfall erosivity calculations based on the Thiessen polygon method with four rain gauge stations in the Sempor Reservoir Catchment Area. Kedungwringin, Sampang, Sempor and Somagede stations showed rainfall erosivities of 2,467.21, 2,437.48, 2,176.53 and 2,828.84 MJ mm $ha^{-1} h^{-1} a^{-1}$, respectively. Rainfall tends to have a maximum destructive impact from January to March and from October to December, during which the erosivity is substantially higher than that during April–September.

Also, it was found that rainfall erosivity has a corresponding pattern to monthly rainfall. As seen in Figure 3, the darker the blue colour on the chart, the higher the rainfall erosivity. The high values are at the beginning and end of the year, and the lighter shows the lowest at midyear. Moreover, it indicates that monsoons control the rainfall in the catchment area. Like most regions in southern Indonesia, the catchment area sees one peak of rainfall from November to March, as influenced by the humid west monsoon, and one trough from May to September due to the dry east monsoon (Aldrian, Susanto 2003). Wheeler et al. (2005) explained that Java Island receives the highest rain from November to March due to convective rain from the formation of cumulonimbus clouds.

Morphologically, the catchment area originates from structural landscape. This landscape comprises river valleys, colluvial plains, lower, middle and upper slopes of structural hills, and ridges or hillcrests. Each landform unit in the catchment area represents one K index.

Table 4 shows the K index values for existing landforms and their determinants, including particle percentage (M) and numerical codes for organic matter content (a), soil structure (b) and soil permeability (c). The soil erodibility value in the

Sempor Reservoir Catchment Area was derived from Fitryady (2008) and Rachma (2019) that used 6 soil samples on each landform. The landform map and soil sampling points are visualised in Figure 4.

Structural hillcrests had the lowest K value. One of the reasons is its substantially lower M value than other landforms. Low M values can be linked to the high clay content in the soil texture. Clay particles have a high adhesion capacity, making them stick tightly together to form large solid aggregates that are resistant to detachment and movement (Jiang et al. 2020). By contrast, colluvial plains and the middle slope of structural hills had the highest M values. Both landforms have the most easily eroded soils in the catchment area due to their low clay and high silt contents (Zehetner, Miller 2006).

Structural hillcrests had the highest organic content (a value). More organic matter increases soil aggregation. This will improve infiltration capacity and decrease surface runoff, reducing the release of soil particles due to raindrops and runoff (Yang et al. 2018). High organic matter in this landform is also attributable to the high clay percentage in soils. There is a positive correlation

Table 3. Rainfall erosivity (R) in the Sempor Reservoir Catchment Area based on rainfall weighting.

Rain station	Rainfall erosivity [R]	Area [km²]	R × Area
Kedungwringin	2,467.21	16.18	39,915.92
Sampang	2,437.48	18.27	44,527.47
Sempor	2,176.53	3.85	8,390.13
Somagede	2,828.84	2.33	6,601.82
Total		40.63	99,435.35
Rainfall erosivity (R) of the reservoir catchment area [MJ mm ha⁻¹ h⁻¹ a⁻¹]			2,447.04

Table 4. Soil erodibility (K) in the Sempor Reservoir Catchment Area.

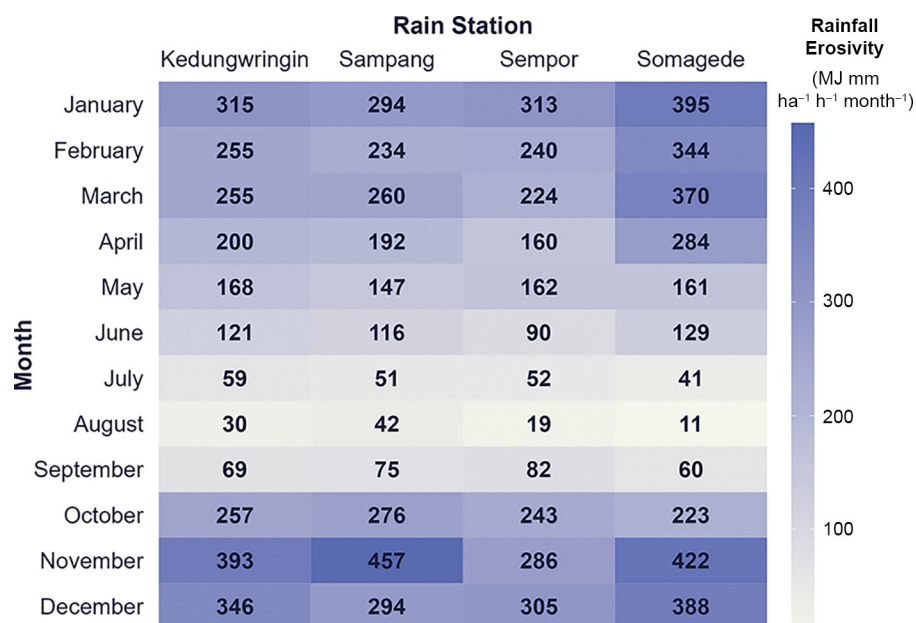| Landform	Texture [%]			M	a	b	c	K
	Sand	Silt	Clay					
River valley	31	37	32	4,624	4.31	3	4	0.39
Colluvial plain	27	64	7	8,463	3.12	2	4	0.76
Lower slope	25	36	39	3,691	4.05	3	1	0.23
Middle slope	20	72	8	8,464	2.62	2	5	0.83
Upper slope	44	31	25	5,625	3.86	2	2	0.38
Hillcrest	10	20	70	873	4.50	3	4	0.12

Fig. 3. Monthly rainfall erosivity of the Sempor Reservoir Catchment Area.
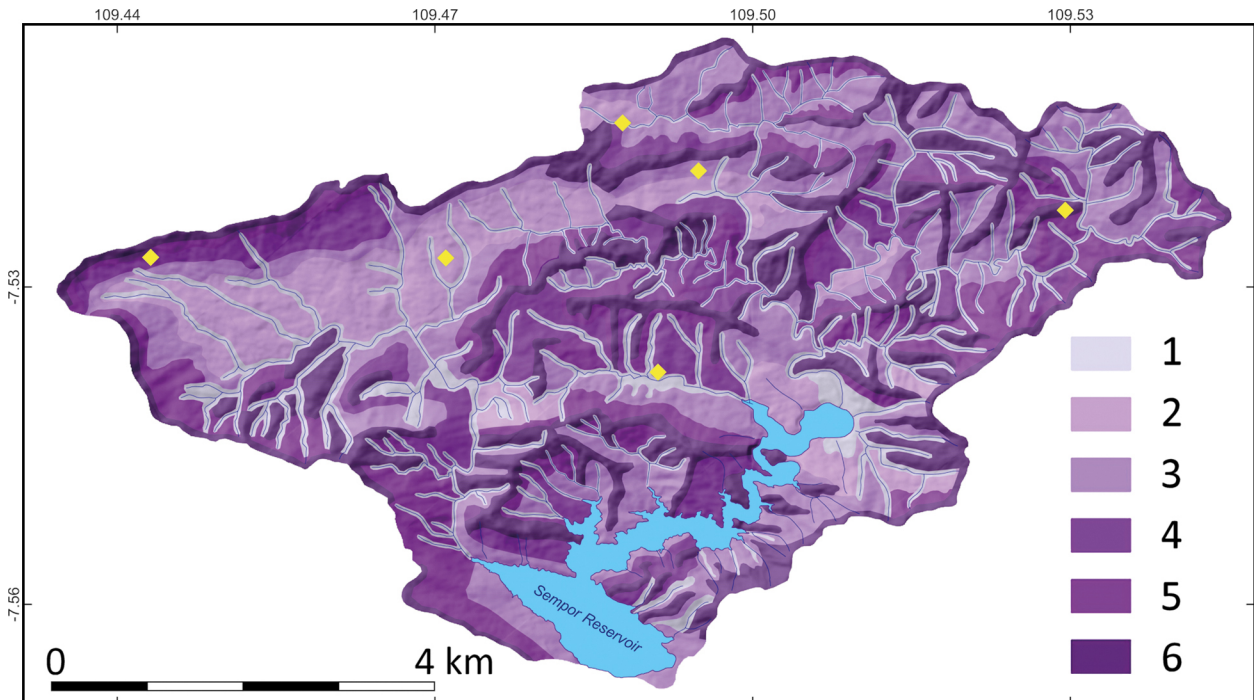
Fig. 4. Landform map and soil sampling points in the Sempor Reservoir Catchment Area. Explanation: yellow squares marked soil samples, landforms: 1 – river valley, 2 – colluvial plain, 3 – lower slope, 4 – middle slope, 5 – upper slope, 6 – hillcrest. Data source: field survey and laboratory analysis by Fitryady (2008) and Rachma (2019).

between organic matter and clay (Sirjani et al. 2019) because clay particles have a large surface area to absorb more organic matter (Qu et al. 2023). Conversely, soils with less clay have lower organic content, such as colluvial plains and the middle slopes of structural hills. However, the same case does not apply to the river valleys in the catchment area. Even though their soil texture has a lower clay percentage than silt and sand, they have nearly as high organic content as hillcrests. The main reason is that river valleys are the potential site for depositing nutrients from sediments entrained by the flow (DeLuca et al. 2013).

Soil permeability differs across the five landforms and shows no regular pattern. The middle slope had the highest b value at code 5, meaning that soil particles allow water to pass slowly at about 0.5 to 2 cm·h^{-1}. Soils with a high proportion of silt have low permeability and resistance to detachment (O'Geen 2006). By contrast, the lower slopes of structural hills had the lowest b value, indicating rapid permeability. This can be linked to the landform's high organic content because there is a generally positive correlation between soil permeability and organic matter (Mulyono et al. 2019). Some exceptions include river valleys and structural hillcrests that have organic matter in large concentrations but transmit water slowly. Table 5 shows variations in slope LS expressed as LS values. The Sempor Reservoir Catchment Area is dominated by 35–50% slope gradients, indicating hilly topography with a very steep composition. Moreover, it has no areas with flat

Table 5. LS classification in the Sempor Reservoir Catchment Area.

Slope [%]	Slope classification	Length and steepness LS	Area [ha]	Percentage [%]
5–15	II	1.20	307.59	7.57
15–35	III	4.25	1,178.64	29.01
35–50	IV	9.50	1,501.23	36.94
>50	V	12.00	1,076.03	26.48
Total			4,063.50	100.00

Table 6. CP in the Sempor Reservoir Catchment Area.

Land use	C	Conservation management	P	Crop management and soil conservation CP	Area [ha]	Percentage [%]
Conservation forest	0.001	No conservation	1.00	0.001	1,373.11	33.8
Plantation forest	0.2	No conservation	1.00	0.2	627.66	15.4
Mixed cropland	0.1	No conservation	1.00	0.1	957.50	23.6
Settlement	1	No conservation	1.00	1	378.06	9.3
Paddy field	0.01	Traditional terraces	0.40	0.004	291.32	7.2
		No conservation	1.00	0.01	37.92	0.9
Dryland farming	0.7	Contour farming (9–20%)	0.75	0.525	130.47	3.2
		Contour farming (>20%)	0.90	0.63	267.46	6.6
Total					4063.50	100.0

terrain or 0–5% slopes. Very steep topography increases the proportion of extreme erosion in total erosion events. As a result, topsoil loses more organic matter quickly, leaving soils with low adhesion and high proneness to erosion (Zhu et al. 2022). The steeper the slope, the faster the sediment movement and the higher the erosion potential (Zhang, Yu 2023).

Land-use response to erosion is expressed as a function of vegetative cover or crop management (C) and soil conservation (P). Table 6 shows CP values as components of erosion potential in the catchment area. Vegetated land usually has a low C index because it is resistant to erosion, for some plant or crop species can affect rainfall partitioning and water flow through interception, infiltration, water absorption and by covering or protecting soil aggregates (Suprayogi et al. 2013). Accordingly, conservation forests were considered the most erosion-resistant land-use type because of the lowest C index (0.001). Plantation forests have a higher C (0.2) because they constitute the product of anthropogenic interventions that most likely cause increased runoff and soil loss (Xiong et al. 2019).

Mixed cropland has a lower C index than dryland farming because crops are planted in a higher density in the former than in the latter. Vegetation plays a crucial role in reducing raindrops' kinetic energy and particle removal from soil aggregates (Satriagasa, Suryatmojo 2020). With wider crop spacing, a larger surface area is exposed to raindrops. Raindrops will fall directly onto the ground without being slowed down by parts of plants. Therefore, compared to forests with high vegetation density, mixed cropland and dryland farming produce more significant surface runoff due to low interception (Zhu et

al. 2022). Further, settlements have the highest C value because they are generally not covered by vegetation. Without vegetation, no objects reduce the flow rate of surface runoff (Hidayah et al. 2022). Information on soil conservation (P) is often scarce or difficult to obtain as it combines detailed data from numerous sources on various scales (Patil 2018). Therefore, the unit of analysis for P calculation is frequently merged with the C index.

Nearly all paddy fields in the reservoir catchment area are traditionally terraced. This engineering can conserve soil better than non-terraced fields as it reduces the amount and speed of surface runoff, thus providing more opportunities for the ground to absorb more water (Arsyad 2010). The soil structure becomes stable with the destructive energy of surface runoff being dissipated (Sutrisno et al. 2011).

Another soil conservation measure is contour farming, i.e., planting crops according to contour lines, as found in non-irrigated fields in the catchment area. Contour farming creates buffer rows that slow runoff, and vegetation on the contour strips can filter and trap sediment effectively (Kuok et al. 2013). Nevertheless, traditional terraces are considered better for soil conservation because they increase the infiltration rate and dissipate the destructive energy of runoff (Idjudin 2011).

Figure 5 presents the distributions of R, K, LS and CP factors in the Sempor Reservoir Catchment Area. These data were overlaid to produce the annual erosion rate (Fig. 6). The 2011 Ministerial Regulation classifies erosion susceptibility into five classes according to erosion rates. Table 7 shows the areal percentage of each susceptibility level in the study area.
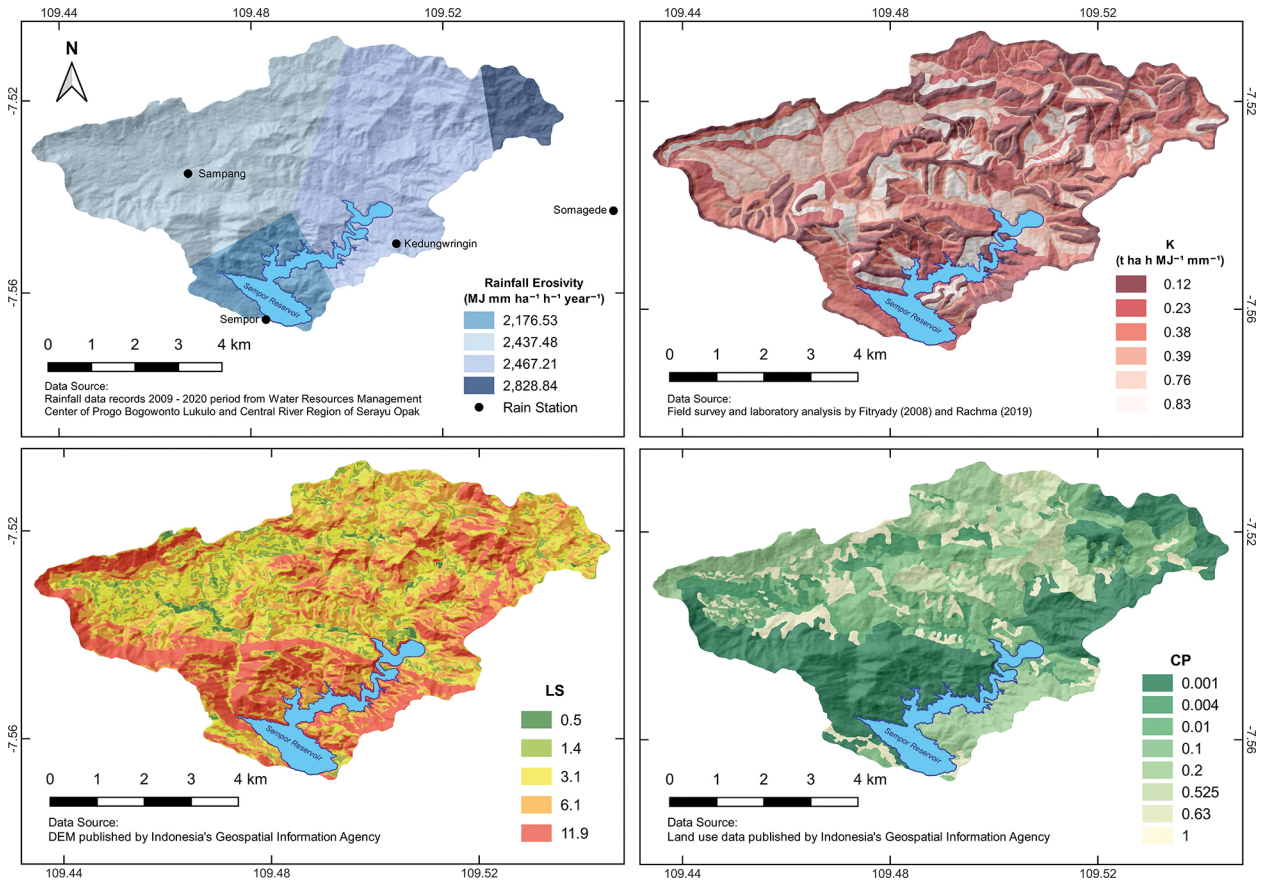
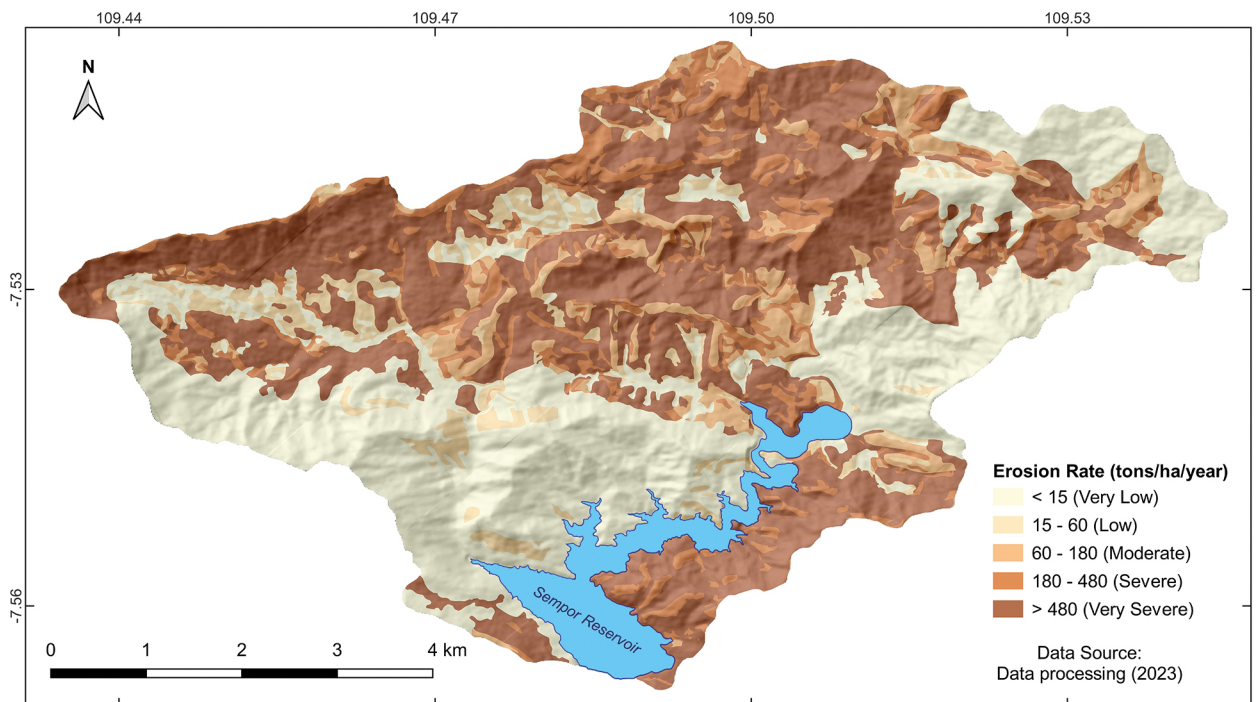Fig. 5. Parameters used in estimating erosion potential with the USLE model.

Fig. 6. Annual erosion rate distribution in the Sempor Reservoir Catchment Area using the USLE model.

Table 7. Distribution of erosion susceptibility in the Sempor Reservoir catchment.

Susceptibility level	Erosion rate [t · ha^{-1} · a^{-1}]	Area [km^2]	Percentage [%]
Very low	<15	16.098	39.62
Low	15–60	3.820	9.40
Moderate	60–180	5.002	12.31
Severe	180–480	6.157	15.15
Very severe	>480	9.559	23.52
Total		40.635	100.00

Sempor Reservoir's morphometry

Echo sounding recorded the depth of the reservoir at 243 points (Fig. 7, see the dots). The depth information was transformed into elevation data to determine the reservoir's volume or capacity at every elevation. Then, the location of each point was used to interpolate the data in m a.s.l. into a raster area. Spatial interpolation with empirical Bayesian kriging was performed by ArcGIS software using the Geostatistical Analyst feature. This interpolation technique was selected based on the pre-determined root mean square error (RMSE). In concept, RMSE compares original (observed)

values with interpolated (predicted) values (Meng et al. 2013). Slight differences between the two values are represented by low RMSE, which indicates that the tested model is the most reliable in predicting values (Mutaqin et al. 2019).

The simple linear regression analysis of the observed and predicted values showed $R^2 = 0.917$, suggesting a strong correlation. The closer the R^2 is to 1, the better the designed interpolation performs (Motovilov et al. 1999). The NSE test produced a coefficient of 0.87, which can be categorised as very good, meaning that the predicted data are accepted and that the evaluated model performs as desired (Moriasi et al. 2007). Another cross-validation analysis showed a MAPE of 13.03%. This MAPE value indicates an interpolation model with good performance (Ali, Abustan 2014).

Using the empirical Bayesian kriging, an elevation contour map was obtained. It shows that the reservoir is located at 42–65 m a.s.l. In addition, the depth data are visualised as a bathymetry map in Figure 8. The darker the blue colour on the map, the deeper the area. The deepest points are concentrated in the middle of the reservoir,
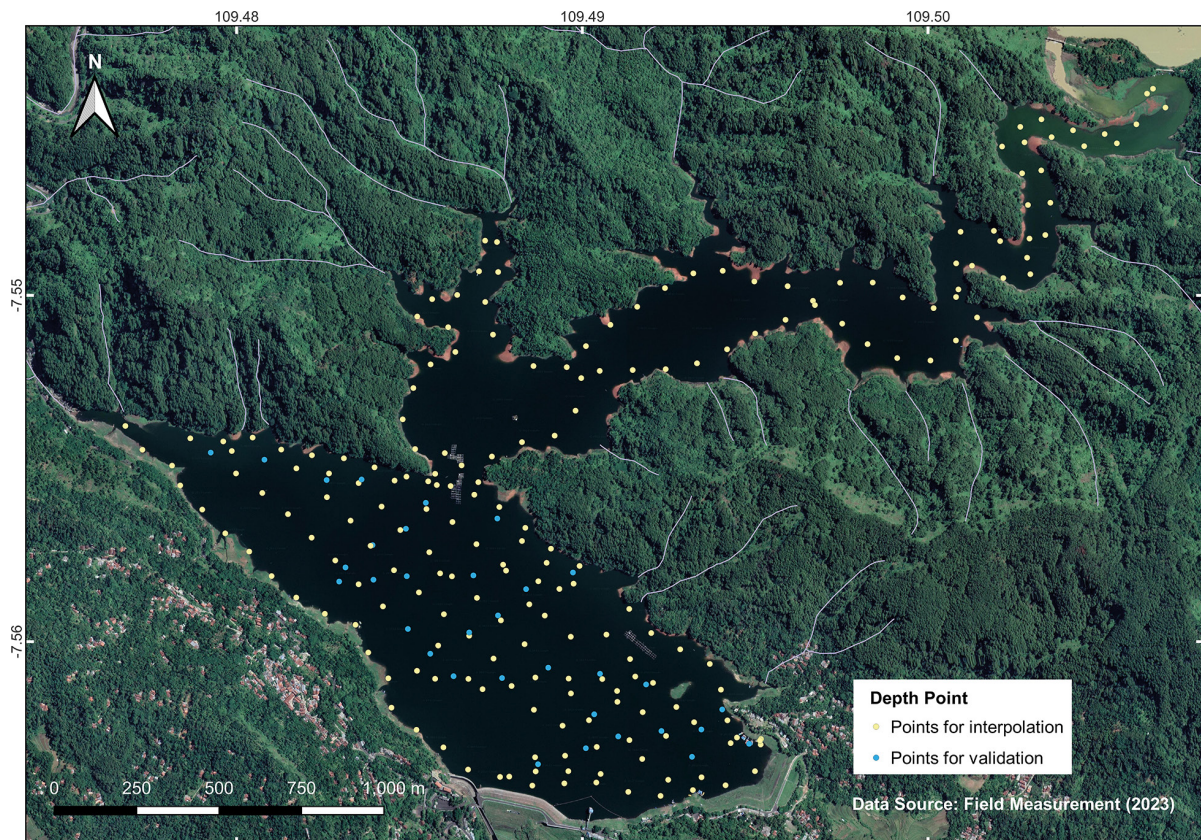

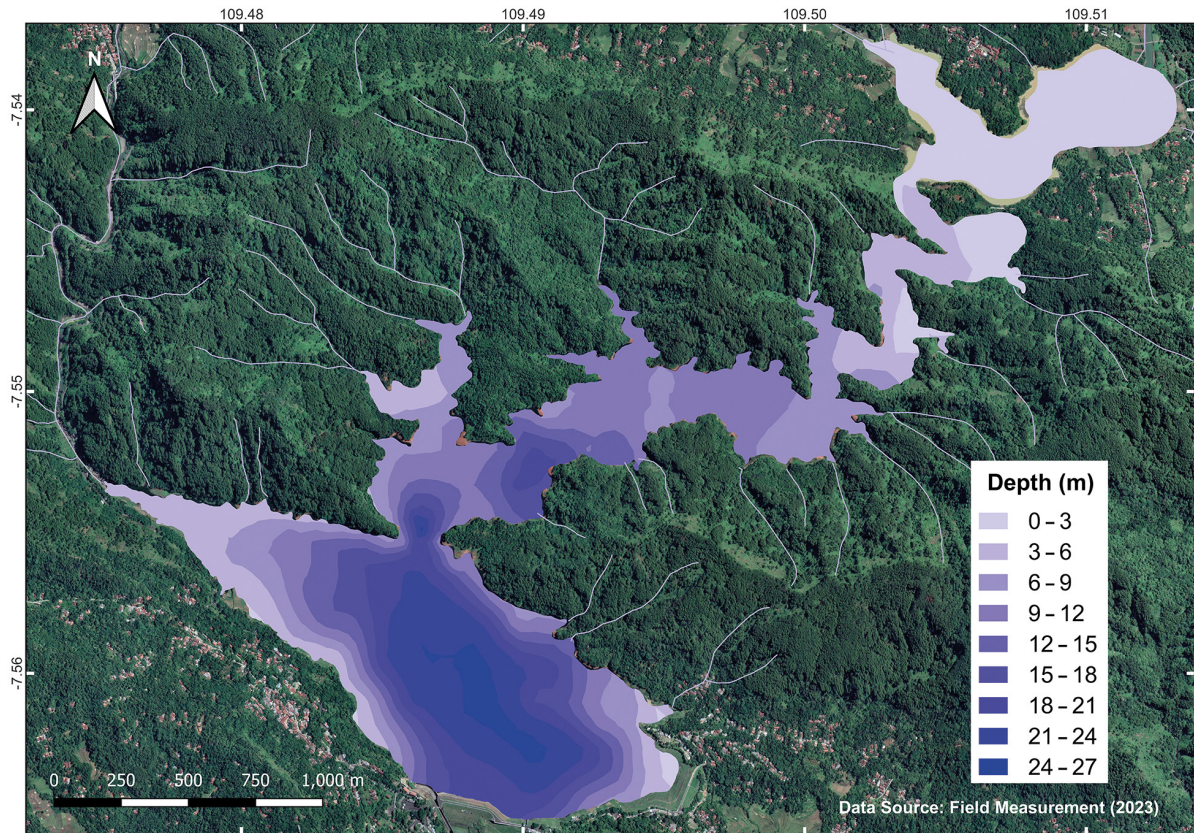Fig. 7. Echo sounding measurement points to record the depth of the Sempor Reservoir.

Fig. 8. Depth contour of the Sempor Reservoir interpolated using empirical Bayesian kriging.

which is close to the outlet. Areas closer to the inlet are shown in lighter blue, illustrating shallower depth.

Interpolated contours were used to determine the inundation area at each elevation, which was further analysed to calculate the reservoir's volume or capacity. The broadest inundation area was 1,971,247.46 m² at 65 m a.s.l., with a reservoir capacity of 23,090,500.45 m³. The inundation area and the dead storage capacity at 43 m a.s.l. were 193,028.93 m² and 155,680.22 m³, respectively.

Sedimentation

Trap efficiency

TE was calculated to determine the ability to trap sediments transported into the Sempor Reservoir. It depends on the reservoir's capacity

Table 8. Monthly discharge of the Sempor Reservoir.

Month	Monthly discharge [mln m³ · month⁻¹]					
	2017	2018	2019	2020	2021	Average
January	16.550	14.309	17.586	13.622	17.695	15.952
February	11.238	15.589	9.324	12.242	15.549	12.788
March	4.765	14.807	10.392	20.843	9.117	11.985
April	11.047	8.404	2.685	6.525	7.566	7.245
May	1.168	0.716	1.713	8.857	9.502	4.391
June	0.884	2.237	0.094	2.039	3.228	1.696
July	0.009	0.922	0.033	0.386	5.191	1.308
August	0.292	0.010	0.596	0.581	0.317	0.359
September	2.000	0.009	–	0.973	1.482	1.116
October	4.415	0.003	0.033	24.668	4.568	6.737
November	10.140	11.840	1.071	26.127	10.569	11.949
December	13.430	0.229	3.768	18.865	15.547	10.368
Annually discharge [mln m³·a⁻¹]						85.897

and annual inflow discharge. Table 8 lists the monthly inflow discharge from 2017 to 2021, with a total annually inflow of 85.897 million m³. Total annually inflow was later combined with reservoir capacity derived from echo sounding in 2023 (23,090,500.45 m³) to obtain TE using the modified Brune formula.

As seen in Table 9, the Sempor Reservoir had 90.09% TE. It means 90.09% of the total sediment entering the reservoir will be deposited. TE is one of the parameters used to estimate the sedimentation rate.

Table 9. Trap efficiency (TE) of the Sempor Reservoir.

Reservoir capacity [m³]	Annually discharge [mln m³ · a⁻¹]	TE [%]
23,090,500.45	85.897	90.09

Sedimentation rate

It is unlikely that all erosion products flow into the reservoir. To calculate the fraction that does, the SDR was used. As Olii et al. (2018) mentioned, the Sempor Reservoir Catchment Area has an SDR of 0.2, meaning that from the erosion potential in the catchment area, 20% is transported into the reservoir. Based on erosion modelling with the USLE method, the erosion potential is 3,405,353.86 t·a⁻¹. Laboratory analysis showed sediments with a specific gravity of 1.99 t·m⁻³. As a result, the sedimentation rate is 681,070.7 t·a⁻¹ or 343,108.7 m³·a⁻¹. Considering the previously calculated TE, total solid particles deposited in the reservoir are 90.09% of the sedimentation rate, i.e., 613,576.66 t·a⁻¹ or 309,106.63 m³·a⁻¹.

As seen in Table 10, the actual sedimentation rate was determined by comparing the dead storage capacities in two different years. In this research, the dead storage capacity in 2013 was obtained from the main station of Serayu-Opak Watershed, while the 2023 capacity was calculated from field-derived data. Any change in dead storage capacity is interpreted as the actual annual sedimentation rate for ten years.

Useful life of the Sempor Reservoir

The useful life of the Sempor Reservoir was derived from actual and potential sedimentation rates, as presented in Table 11. The Sempor Reservoir was planned to have an effective age of 50 years since its construction, thus expected to perform optimally until 2028 (Julia 2017). After comparing the capacities, the estimation confirmed that the reservoir's useful life or optimal performance would last until 2028 or according to the initial design life.

Table 11. Estimated remaining years of the useful life of the Sempor Reservoir.

	Actual	Potential
Dead storage [m³]	155,680.22	
Sedimentation rate [m³·a⁻¹]	33,903.275	309,106.630
Remaining useful life [year]	4.59	0.50

However, there are always room where predictions are not necessarily in line with actual conditions. Therefore, the potential sedimentation rate that assumes all sediments will be deposited at dead storage capacity was also calculated. In actuality, sediments settle throughout the bottom of the reservoir (Putra et al. 2019). Therefore, the potential sedimentation rate is probably slower, and the remaining useful life would be >0.5 years. On the contrary, the useful life can also end earlier than in the next 4.59 years due to the flow dynamics that cause sediments at elevations above dead storage capacity to flow more quickly towards it. Therefore, the actual sedimentation rate can be substantially faster.

The remaining useful life can also be >0.5 years. The reason is that this estimate does not consider sediment control structures as a conservation measure that can reduce erosion and sedimentation rates in the reservoir and its catchment area. However, the erosion potential produced using the USLE model is also possibly overestimated (Dariah et al. 2004) because it only sees rainfall as erosion control but does

Table 10. Actual sedimentation rate of the Sempor Reservoir.

Dead storage in 2013 [m³]	Dead storage in 2023 [m³]	Dead storage change [10 years m³]	Actual Sedimentation Rate [m³·a⁻¹]
494,712.98	155,680.22	339,032.75	33,903,275

not incorporate its partitioning or conversion into runoffs (Kinnell 2016, Meinen, Robinson 2021). Therefore, future research should analyse the erosion potential more specifically by incorporating, for instance, hydrological studies and validation in the field.

Conclusions

The erosion rate each month will correspond to the amount of rainfall in that particular month. Monthly temporal variations indicate that the highest and lowest monthly erosions in the Sempor Reservoir Catchment Area occur in November (the month with the highest rainfall erosivity) and August (the month with the lowest rainfall erosivity), respectively. Spatial variations reveal that the dominance of erosion rates classified as very light occurs on the west and northeast sides of the reservoir, which is related to land use in these areas, characterised as conservation forests. Erosion rates classified as heavy to very heavy are distributed in the central and northern parts of the watershed. Mixed cropland and dryland farming associated with steep slopes pose a high erosion potential.

The substantial annual erosion, as determined by the USLE model, has resulted in a shortened useful life of the Sempor Reservoir due to significant sedimentation. However, the useful life of the Sempor Reservoir still has the potential to exceed the estimate based on erosion potential, which is 0.5 years. The estimation of erosion potential also has the potential to experience overestimate results. The estimation of erosion potential does not consider the existence of conservation efforts in the form of sediment control buildings. Sediment control buildings are considered to be a factor that can suppress the rate of erosion and sedimentation in the Sempor Reservoir catchment area.

In the meantime, the conservation efforts undertaken in the Sempor Reservoir Catchment Area are considered quite good as the Sempor Reservoir is still capable of operating close to its planned useful life, which extends until the year 2028 based on the actual sedimentation rate (4.59 years). This is reflected in the land use within the Sempor Reservoir Catchment Area, which is still predominantly covered by forests.

Conservation forests are considered to have the highest resistance to erosion due to their canopy's ability to reduce rainfall impact. However, plantation forests have a relatively high erosion potential because land impacted by anthropogenic activities can result in surface runoff. The plantation forest on the eastern side of the reservoir has a significant erosion potential. Therefore, conservation efforts in the Sempor Reservoir Catchment Area still need to be carefully considered.

Acknowledgements

Author's contribution

Satrio Budiman: conceptualisation, methodology, data collection, data analysis, result interpretation and draft preparation. Slamet Suprayogi: conceptualisation, methodology and critical manuscript revision. All authors have reviewed the results and approved the final version of this manuscript.

References

Ahmad N.S.B.N., Mustafa F.B., Yusoff S.Y.M., Didams G., 2020. A systematic review of soil erosion control practices on the agricultural land in Asia. *International Soil and Water Conservation Research* 8: 103–115. DOI 10.1016/j.iswcr.2020.04.001.

Aldrian E., Susanto R.D., 2003. Identification of three dominant rainfall regions within Indonesia and their relationship to sea surface temperature. *International Journal of Climatology* 23(12): 1435–1452. DOI 10.1002/joc.950.

Ali M.H., Abustan I., 2014. A new novel index for evaluating model performance. *Journal of Natural Resources and Development* 4: 1–9. DOI 10.5027/jnrd.v4i0.01.

Arsyad S., 2010. *Konservasi Tanah dan Air*. IPB Press, Bogor.

Asdak C., 2020. *Hidrologi dan Pengelolaan Daerah Aliran Sungai*. Gadjah Mada University Press, Yogyakarta.

Chang K.T., 2007. *Introduction to geographic information system*. 4th edn, McGraw-Hill, New York.

Christanto N., Setiawan M.A., Nurkholis A., Istiqomah S., Sartohadi J., Hadi M.P., 2018. Sedimentation rate analysis at the upper Serayu watershed using the SWAT model. *Majalah Geografi Indonesia* 32(1): 50–58.

Dargahi B., 2012. Reservoir sedimentation. In: Bengtsson, L., Herschy, R.W., Fairbridge, R.W. (eds), *Encyclopedia of lakes and reservoir*. Springer, Amsterdam.

Dariah A., Subagyo Tafakresnanto C., Marwanto S., 2004. *Kepekaan Tanah terhadap Erosi*. Centre for Soil and Agro-Climate Research and Development, Bogor

DeLuca T.H., Zackrisson O., Bergman I., Díez B., Bergman B., 2013. Diazotrophy in alluvial meadows of subarctic river systems. *PLOS ONE* 8(11): 1–10. DOI 10.1371/journal.pone.0077342.

El-Swaify S., Dangler E.W., Armstrong C.L., 1982. *Soil erosion by water in the tropics*. College of Tropical Agriculture and Human Resource, University of Hawaii, Honolulu.

Fitryady D., 2008. *Sebaran Jenis Tanah Berdasarkan Jenis Formasi Geologi di Daerah Aliran Sungai (DAS) Waduk Sempor Kabupaten Kebumen*. Master Thesis. Universitas Gadjah Mada. Yogyakarta.

Gerrard A.J., 1981. *Soils and landform*. George Allen and Unwin, London.

Gill M.A., 1979. Sedimentation and useful life of reservoirs. *Journal of Hydrology* 44(1–2): 89–95. DOI 10.1016/0022-1694(79)90148-3.

Goovaerts P., 2000. Geostatistical approaches for incorporating elevation into the spatial interpolation of rainfall. *Journal of Hydrology* 228(3): 113–129. DOI 10.1016/S0022-1694(00)00144-X.

Haregewyn N., Melesse B., Tsunekawa A., Tsubo M., Meshesha D., Balana B.B., 2012. Reservoir sedimentation and its mitigating strategies: A case study of Angereb reservoir (NW Ethiopia). *Journal of Soils Sediments* 12(1): 291–305. DOI 10.1007/s11368-011-0447-z.

Hidayah E., Widiarti W.Y., Ammarulsyah A.R., 2022. Flood vulnerability zoning with geographic information system in Kaliputih sub-watershed, Jember District. *Jurnal Teknik Pengairan* 13(2): 273–282.

Idjudin A.A., 2011. The role of land conservation roles in plantation management. *Jurnal Sumberdaya Lahan* 5(2): 103–116.

Indonesia Ministry of Forestry, (2009). Peraturan Menteri Kehutanan Republik Indonesia Nomor P. 32/Menhut-Ii/2009 Tentang Tata Cara Penyusunan Rencana Teknik Rehabilitasi Hutan dan Lahan Daerah Aliran Sungai (Rtkrhl-DAS) (Ministerial Regulation No. P.32/menhut-ii/2009 on Procedures for Preparing Engineering Plans for Forest and Land Rehabilitation in Watersheds). Jakarta.

Indonesia Ministry of Forestry, 2011. Ministerial Regulation No. P.7/DAS-V/2011 on Technical Guidelines for the Standard Operating Procedure (SOP) System for Flood and Landslide Mitigation. Jakarta.

Indonesia Ministry of Public Works and Settlement, 2017. *Modul Operasi Waduk*. Centre for Education and Training of Water Resources and Construction, Bandung.

Jiang Q., Zhou P., Liao C., Liu Y., Liu F., 2020. Spatial pattern of soil erodibility factor (K) as affected by ecological restoration in a typical degraded watershed of Central China. *Science of the Total Environment* 749: 1–12. DOI 10.1016/j.scitotenv.2020.141609.

Julia H., 2017. The significance of check dam construction scenarios in slowing sedimentation rates in the Sempor reservoir. *Agrium* 21(1): 78–88. DOI 10.30596/agrium.v21i1.1490.

Kebumen Agriculture and Food Service Office, 2021. *Agriculture statistics book 2020*. Agriculture and Food Service Office, Kebumen.

Keshavarzi A., Kumar V., Bottega E.L., Rodrigo-Comino Jesús., 2019. Determining land management zones using pedo-geomorphological factors in potential degraded regions to achieve land degradation neutrality. *Land* 8(6): 1–14. DOI 10.3390/land8060092.

Kinnell P.I.A., 2016. Comparison between the USLE, the USLE-M, and replicate plots to model rainfall erosion on bare fallow areas. *Catena* 145: 39–46. DOI 10.1016/j.catena.2016.05.017.

Kuok K.K.K., Mah D.Y.S., Chiu P.C., 2013. Evaluation of C and P factors in universal soil loss equation on trapping sediment: Case study of Santubong river. *Journal of Water Resource and Protection* 5(12): 1149–1154. DOI 10.4236/jwarp.2013.512121.

Li Z.W., 2014. Land use impacts on soil detachment capacity by overland flow in the Loess Plateau, China. *Catena* 124: 9–17. DOI 10.1016/j.catena.2014.08.019.

Lihawa F., 2017. Daerah Aliran Sungai Alo: Erosi, Sedimentasi, dan Longsoran. Deepublish, Yogyakarta.

Main Station of Serayu-Opak Watershed, 2020. *Tingkatkan Nilai Fungsi Waduk Sempor, BBWS Serayu Opak Akan Lakukan Pengerukan Sedimen*. https://sda.pu.go.id/balai/bbwsserayuopak/tingkatkan-nilai-fungsi-waduk-sempor-bbws-serayu-opak-akan-lakukan-pengerukan-sedimen/. Retrieved by Satrio Budiman on 16 August 2022.

Marhaendi T., 2013. Sedimentation management strategies for reservoirs. *Jurnal Techno* 14(2): 29–41.

Meinen B.U., Robinson D.T., 2021. Agricultural erosion modelling: Evaluating USLE and WEPP field-scale erosion estimates using UAV time-series data. *Environmental Modelling and Software* 137: 1–10. DOI 10.1016/j.envsoft.2021.104962.

Meng Q., Liu Z., Borders B.E., 2013. Assessment of regression kriging for spatial interpolation – comparisons of seven GIS interpolation methods. *Cartography and Geographic Information Science* 40(1): 28–39. DOI 10.1080/15230406.2013.762138.

Moriasi D.N., Arnold J.G., Liew M.W., Van Bingner R.L., Harmel R.D., Veith T.L., 2007. Model evaluation guidelines for systematic quantification of accuracy in watershed simulations. *American Society of Agricultural and Biological Engineers* 50(3): 885–900. DOI 10.13031/2013.23153.

Motovilov Y.G., Gottschalk L., Engeland K., Rodhe A., 1999. Validation of a distributed hydrological model against spatial observations. *Agricultural and Forest Meteorology* 98: 257–277. DOI 10.1016/S0168-1923(99)00102-1.

Mulyono A., Rusydi A.F., Lestiana H., 2019. Soil permeability of various land use types in coastal alluvial soils in Cimanuk watershed, Indramayu. *Jurnal Ilmu Lingkungan* 17(1): 1–6. DOI 10.14710/jil.17.1.1-6.

Mutaqin B.W., Lavigne F., Sudrajat Y., Handayani L., Lahitte P., Virmoux C., Hiden, Hadmoko D.S., Komorowski J.C., Hananto N.D., Wassmer P., Hartono, Boillot-Airaksinen K., 2019. Landscape evolution on the Eastern Part of Lombok (Indonesia) related to the 1257 CE eruption of the Samalas Volcano. *Geomorphology* 327: 338–350. DOI 10.24114/jg.v13i2.21526.

Nagle G., Covich A., Fahey T.J., Lassoie J.P., 1999. Management of sedimentation in tropical watersheds. *Environmental Management* 23(4): 441–452. DOI 10.1007/s002679900199.

Nugraha A.R., Saputro S., Purwanto., 2013. Bathymetry mapping and tidal analysis to determine floor elevation of Pier 136 at the Mahakam River Estuary, Sanga-Sanga, East Kalimantan. *Jurnal Oseanografi* 2(3): 238–244.

O'Geen A.T., 2006. *Erodibility of agricultural soils, with examples in lake and mendocino counties*. Division of Agriculture and Natural Resources University of California, California.

Olii M.R., Kironoto B.A., Yulistiyanto B., Sunjoto, 2018. Estimating spatially distributed sediment yield using GIS-RUSLE-SEDD model in Catchment of Reservoir in Java. *Proceedings of International Association for Hydro-Environment Engineering and Research (IAHR)-Asia Pacific Division (APD) Congress: Multi-Perspective Water for Sustainable Development*. IAHR-APD, Yogyakarta.

Oliveira P.T.S., Wendland E., Nearing M.A., 2012. Rainfall erosivity in Brazil: A review. *Catena* 100: 139–147. DOI 10.1016/j.catena.2012.08.006.

Park S.J., Burt T.P., 2002. Identification and Characterization of Pedogeomorphological Processes on a Hillslope. *Soil Science Society of America Journal* 66(6): 1897–1910. DOI 10.2136/sssaj2002.1897.

Patil R.J., 2018. *Spatial techniques for soil erosion estimation*. In: Spatial Techniques for Soil Erosion Estimation, SpringerBriefs in GIS. Springer, Cham. DOI 10.1007/978-3-319-74286-1_4.

Putra D.S., Siwu W.P., Wulandari D.A., 2019. Effects of sedimentation on the function of Karian reservoir. *Jurnal Teknisia* 24(2): 108–116.

Putri M.D., Baskoro D.P.P., Tarigan S.D., Wahjunie E.D., 2017. Characteristics of several soil properties at various slope positions and land uses in upper Ciliwung watershed. *Jurnal Ilmu Tanah dan Lingkungan* 19(2): 81–85. DOI 10.29244/jitl.19.2.81-85.

Qu L., Zhu X., Liang Y., Qiu D., Zhang Q., Liang Y., 2023. Spatial variation of soil properties and evaluation of the risk of soil erodibility on a river alluvial and marine sedimentary plain in Eastern China. *Journal of Soils and Sediments* 23: 2106–2119. DOI 10.1007/s11368-023-03460-8.

Rachma H.A., 2019. *Estimasi Umur Layanan Waduk Sempor sebagai Suplai Irigasi*. Undergraduate Thesis. Universitas Gadjah Mada. Yogyakarta.

Reddy M.G.R., Reddy G.P.O., Maji A.K., Nageshwara Rao K., 2003. Landscape analysis for pedo-geomorphological characterization in part of Basaltic Terrain, Central India using remote sensing and GIS. *Journal of The Indian Society of Remote Sensing* 31(4) 271–282. DOI 10.1007/BF03007347.

Renard K.G., Foster G.R., Weesies G.A., McCool D.K., Yoder D.C., 1997. Predicting soil erosion by water a guide to conservation planning with the revised universal soil loss equation (RUSLE). U.S. Department of Agriculture, Washington D. C.

Satriagasa M.C., Suryatmojo H., 2020. Effectiveness of elephant grass cover (*Pennisetum purpureum*) in mitigating soil erosion by rainwater. *agriTECH* 40(2): 141–149. DOI 10.22146/agritech.50290.

Schleiss A.J., Franca M.J., Juez C., De Cesare G., 2016. Reservoir sedimentation. *Journal of Hydraulic Research* 54(6): 595–614. DOI 10.1080/00221686.2016.1225320.

Sirjani E., Sameni A., Moosavi A.A., Mahmoodabadi M., Laurent B., 2019. Portable wind tunnel experiments to study soil erosion by wind and its link to soil properties in the Fars Province, Iran. *Geoderma* 333: 69–80. DOI 10.1016/j.geoderma.2018.07.012.

Sisinggih D., Wahyuni S., Hidayat F., 2021. *Sedimentasi Waduk*. Universitas Brawijaya Press, Malang.

Subramanya K., 2008. *Engineering hydrology*. Tata McGraw-Hill Publishing Company Limited, New Delhi.

Sumiahadi A., Acar R., 2019. Soil Erosion in Indonesia and Its Control. *Proceeding book of international symposium for environmental science and engineering research (ISESER)*. Necmettin Erbakan University, Konya.

Suprayogi S., Purnama Ig.L.S., Darmanto D., 2013. *Pengelolaan Daerah Aliran Sungai*. Gadjah Mada University Press, Yogyakarta.

Susilo E., 2001. Kajian Efisiensi Tangkapan Sedimen pada Beberapa Waduk di Jawa. *Master Thesis*. Diponegoro University. Semarang.

Sutrisno J., Sanim B., Saefuddin A., Sitorus S.R.P., 2011. Erosion and sedimentation predictions for Keduang sub-watershed, Wonogiri District. *Media Konservasi* 16(2): 78–86.

Tian Y., Xu Y.P., Yang Z., Wang G., Zhu Q., 2018. Integration of A Parsimonious Hydrological Model with Recurrent Neural Networks for Improved Streamflow Forecasting. *Water* 10(11): 1–17. DOI 10.3390/w10111655.

U.S. Department of The Interior, 2006. *Erosion and sedimentation manual* (Issue November). Bureau of Reclamation, U.S. Department of The Interior, Washington D. C.

United Nations Statistic Division, 2017. Manual on the basic set of environmental statistics of the FDES 2013: Water resources statistic. United Nations, New York.

Van Bemmelen R.W., 1949. The geology of Indonesia: General geology of Indonesia and adjacent archipelagoes. Government Printing Office, The Hague, Jakarta.

Wantzen K.M., Mol J.H., 2013. Soil erosion from agriculture and mining: A threat to tropical stream ecosystems. *Agriculture* 3: 660–683. DOI 10.3390/agriculture3040660.

Wheeler M.C., Mcbride J., Lau W.K.M., 2005. Intraseasonal variability in the atmosphere-ocean climate system: Australian-Indonesian monsoon. Springer Berlin Heidelberg, Berlin.

Wischmeier W.H., Smith D.D., 1978. *Predicting rainfall erosion losses: A guide to conservation planning*. U.S. Department of Agriculture, Washington D. C.

Xiong M., Sun R., Chen L., 2019. A global comparison of soil erosion associated with land use and climate type. *Geoderma* 343: 31–39. DOI 10.1016/j.geoderma.2019.02.013.

Yang X., Gray J., Chapman G., Zhu Q., Tulau M., McInnes-Clarke S., 2018. Digital mapping of soil erodibility for water erosion in New South Wales, Australia. *Soil Research* 56(2): 158–170. DOI 10.1071/SR17058.

Zehetner F., Miller W.P., 2006. Erodibility and runoff-infiltration characteristics of volcanic ash soils along an altitudinal climosequence in the Ecuadorian Andes. *Catena* 65(3): 201–213. DOI 10.1016/j.catena.2005.10.003.

Zhang Z., Yu R., 2023. Assessment of soil erosion from an ungauged small watershed and its effect on Lake Ulansuhai, China. *Land* 12(2): 1–15. DOI 10.3390/land12020440.

Zhu Y., Li W., Wang D., Wu Z., Shang P., 2022. Spatial pattern of soil erosion in relation to land use change in a rolling hilly region of Northeast China. *Land* 11(8): 11–17. DOI 10.3390/land11081253.